Environmental Technology & Innovation 28 (2022) 102653

Contents lists available at ScienceDirect

Environmental Technology & Innovation

journal homepage: www.elsevier.com/locate/eti

Formation of phosphine and its effect on phosphorus retention in constructed wetlands: Characteristic and mechanism

Shuo Wang [a], Zhen Hu [a,b,*], Jian Zhang [c], Haiming Wu [a], Huijun Xie [b], Shuang Liang [a], Haodong Hu [a], Fenglin Jin [a]

[a] Shandong Key Laboratory of Water Pollution Control and Resource Reuse, School of Environmental Science & Engineering, Shandong University, Qingdao 266237, PR China
[b] Field Monitoring Station of the Ministry of Education for the East Route of the South-to-North Water Transfer Project, Shandong University, Jinan, 250100, PR China
[c] College of Safety and Environmental Engineering, Shandong University of Science and Technology, Qingdao 266590, PR China

ARTICLE INFO

Article history:
Received 14 January 2022
Received in revised form 2 April 2022
Accepted 2 May 2022
Available online 11 May 2022

Keywords:
Constructed wetlands
Phosphine
Phosphorus cycle
Polylactic acid
Matrix-bound phosphine
Sustainable operation

ABSTRACT

Phosphine (PH_3) is widely present in the atmosphere and plays an essential role in the global phosphorus cycle. However, its source and sink are currently unclear. In this study, the fate and mechanism of PH_3 production in lab-scale constructed wetlands (CWs) were investigated. The results showed that gaseous PH_3 release from CWs mainly occurred in the later stage of the operation cycle. The dissolved PH_3 concentration in the CW effluent varied from 2.73 to 4.08 $\mu g \cdot L^{-1}$, and the matrix-bound PH_3 content in the CWs varied from 2.60 to 16.39 $ng \cdot kg^{-1}$. Moreover, the formation and migration of PH_3 in CWs could increase the proportion of available phosphorus and subsequently increase the phosphorus adsorption capacity by 103.6%. An exogenous electron donor promoted the production of nicotinamide adenine dinucleotide and subsequently increased the production of PH_3. This study revealed a new biological pathway to enhance phosphorus removal by CWs, which should shed light on their sustainable operation.

1. Introduction

Phosphine (PH_3) is a potent reducing agent and has been extensively documented as the gaseous carrier of phosphorus (P) in the global biogeochemical cycle (Chen et al., 2017). To date, PH_3 has been observed in wastewater treatment plants (WWTPs) (Devai et al., 1988), the global atmosphere (Glindemann et al., 2003), soil (Eismann et al., 1997), oceans (Zhu et al., 2011), and other environments (Ding et al., 2005). PH_3 mainly exists in the forms of free gaseous PH_3 (FGP), matrix-bound PH_3 (MBP), and dissolved PH_3 (DP) (Eismann et al., 1997; Glindemann et al., 2005). It is estimated that at least 40,000 tons of PH_3 enter the atmosphere every year, and PH_3 will transform to phosphates under specific conditions and migrate to water bodies or soils through precipitation and deposition, which could accelerate the biogeochemical cycle of P (Fu and Zhang, 2020).

Although P is one of the core elements of life activities, its distribution in ecosystems is not in equilibrium. Excessive P in water will lead to mass algae blooming, resulting in water quality deterioration. Constructed wetland (CW) is an efficient ecological technique for removing P from water bodies. Vymazal (2007) reported that the total phosphorus (TP) removal

* Corresponding author at: Shandong Key Laboratory of Water Pollution Control and Resource Reuse, School of Environmental Science & Engineering, Shandong University, Qingdao 266237, PR China.
E-mail address: huzhen885@sdu.edu.cn (Z. Hu).

https://doi.org/10.1016/j.eti.2022.102653

Nomenclature

Abbreviations

COD	Chemical oxygen demand
CW	Constructed wetland
CW-C	Conventional constructed wetland
CW-P	Polylactic acid particles enhanced constructed wetland
DO	Dissolved oxygen
DP	Dissolved phosphine
Eh	Redox potential
FGP	Free gaseous phosphine
FTD	Flame thermionic detector
GC	Gas chromatograph
HCl-P	Phosphorus extracted by HCl solution
HRT	Hydraulic retention time
MBP	Matrix-bound phosphine
NADH	Nicotinamide adenine dinucleotide
$NaHCO_3$-P	Phosphorus extracted by $NaHCO_3$ solution
NaOH-P	Phosphorus extracted by NaOH solution
NH_4^+-N	Ammonia-nitrogen
NO_2^--N	Nitrite-nitrogen
NO_3^--N	Nitrate-nitrogen
P	Phosphorus
PH_3	Phosphine
PLA	Polylactic acid
PVC	Polyvinyl chloride
Resin-P	Phosphorus extracted by resin
SBBR	Sequencing batch biofilm reactor
TP	Total phosphorus
WWTP	Wastewater treatment plant

rate in all types of CWs varied from 40% to 60%. Adsorption and precipitation by substrates are the primary mechanisms of P removal in CWs (Wu et al., 2015). Many scholars have committed to researching and developing efficient P adsorption substrates over the past decades (Wu et al., 2015). CWs with mine waste (coal gangue, iron ore and manganese ore) could increase the removal of TP by 17–34%, which is attributed to the strong binding mechanism of phosphate with the oxides and hydroxides of Mn, Fe and/or Al that are leached out of mine waste (Wang et al., 2022). CWs coupled to microbial fuel cells filled with alum sludge reduced TP in the effluent by approximately 90% (Yang et al., 2021). The substrates for P removal include natural minerals, industrial by-products and artificial products, which are all used to enhance P removal in CWs (Westholm, 2006). However, after the CW runs for 3–5 years, the problem of substrate adsorption saturation arises, leading to a sharp decline in P removal efficiency (Arias et al., 2001). Blanco et al. (2016) studied the P removal efficiency of CWs filled with steel slag aggregates, and found a gradual decline in P removal efficiency from 99% to 7% with the decline in Ca^{2+} and OH^-. Although the P removal efficiency of CWs can be improved by replacing substrates or by chemical regeneration (Drizo et al., 2002; Pratt et al., 2009), it will significantly increase the operation cost and affect the sustainable operation of CWs.

Recently, a new phosphorus removal process based on biological reduction of phosphate to PH_3 (dephosphorization by gasification) has attracted wide attention in wastewater treatment. Devai et al. (1988) calculated the material balance of P in a wastewater treatment system and found that approximately 25–50% of the P deficit can be explained by the formation of PH_3. Yang et al. (2016) found that in a sequencing batch biofilm reactor (SBBR), the P removal efficiency was 85–94% without excess sludge discharge, and a significant concentration of MBP (3.11 $mg{\cdot}PH_3{\cdot}kg^{-1}$ wet sludge) was detected. Dephosphorization by gasification provides a new possibility for enhancing the P removal of CWs. It is of great significance to clarify the impact of PH_3 on P removal in CWs.

The mechanism of PH_3 formation in nature has been controversial for decades. Some scholars believe that PH_3 formation is associated with microorganisms because various kinds of P compounds can be reduced to PH_3 under the effect of anaerobic bacteria (Han et al., 2002; Roels et al., 2005). However, Glindemann et al. (2005) proposed that PH_3 was generated from rocks via mechanochemical or "tribochemical" weathering. To date, the mechanism of PH_3 production is still unclear, and no study has been conducted to analyze the characteristics and mechanism of PH_3 production in CWs.

In this study, we conducted several constructed wetland microcosms and comprehensively evaluated the characteristics of PH_3 production in CWs, which have been previously neglected. The effect of PH_3 on phosphorus retention was revealed, which provides new insight into phosphorus transformation in CWs. In addition, we have preliminarily clarified the mechanism of PH_3 production by exogenous electron donor supported. Overall, the findings of this study provide new insight into the long-term effective phosphorus removal by CWs.

2. Materials and methods

To investigate the formation characteristics of PH_3 and its effect on phosphorus retention in CWs, a series of CW microcosms were designed and operated at Shandong University, Qingdao, China.

2.1. Experimental set-up

CW microcosms (inner diameter, 24 cm; height, 85 cm) made with polymethyl methacrylate were divided into two groups and operated for 150 d. A perforated PVC tube (length × diameter = 85 cm × 3 cm) was vertically inserted into the CWs for physicochemical index monitoring. The control group was a conventional CW (CW-C) filled with quartz sand (diameter ranging from 0.8 to 1.6 cm), and the treatment group was an enhanced CW (CW-P) filled with quartz sand and 30% (v/v) polylactic acid particles (PLA, diameter 0.5 cm) at depths of 15–60 cm. Synthetic polymers (such as polycaprolactone, polyhydroxyalkanoates and polylactic acid) have historically been added to CWs as electron donors for denitrification (Shen et al., 2015). Lactate is commonly used as a high-energy electron donor for biological reduction processes (Xia et al., 2019). Therefore, PLA was added to CWs to optimize bio-reduction environment. *Iris pseudacorus*, which is widely distributed in the wetlands of northern China and has strong pollution resistance and cold resistance, was planted in the CWs at a density of 70 rhizomes per square meter. After acclimation of plants and microorganisms for 30 d, the formal experiment was conducted.

2.2. Experimental procedures

The CWs were operated under intermittent conditions and were controlled by a solenoid valve and a programmable timer. An intermittent operation strategy for CWs can achieve high pollutant removal efficiency (Zhang et al., 2020). The flooding and draining phases were rhythmically set, including a 0.1 h feeding phase, an 18 h flooding phase, a 0.3 h draining phase, and a 5.6 h idle phase. The hydraulic retention time (HRT) was 24 h. The synthetic water was composed of $C_6H_{12}O_6$, NH_4Cl, KH_2PO_4, and trace elements, which simulated the rural domestic sewage of northern China, and the concentration of P was appropriately increased (Table S1). The inflow concentrations of chemical oxygen demand (COD), TP, and ammonia-nitrogen (NH_4^+-N) were 203.36 ± 3.10 mg·L^{-1}, 5.14 ± 0.11 mg·L^{-1}, and 20.63 ± 0.40 mg·L^{-1}, respectively.

2.3. Phosphine analysis

The gaseous PH_3 released from the CWs was collected using the static closed-chamber method (Zhang et al., 2018). The PH_3 in gas samples was measured using a gas chromatograph (GC-2010 Pro, Shimadzu) equipped with a capillary column (SH-rTX-5, 30 m × 0.32 mm ×0.50 μm, Shimadzu) and a flame thermionic detector (FTD). The gas samples were enriched through an ultralow temperature capillary cryo-trap (Al_2O_3/Na_2SO_4 capillary column) before being injected into the GC. The oven temperature of the GC was 40 °C, and the temperature of the FTD was 250 °C. Nitrogen (N_2) was the carrier gas with a flow rate of 2 mL·min^{-1}. The FTD gases were high purity hydrogen (H_2, 3 mL min^{-1}) and dry air (150 mL·min^{-1}). The detection limit of PH_3 was 0.1 ng·m^{-3}.

The gaseous PH_3 emission fluxes were calculated by the following equation (Han et al., 2011a):

$$F = (dC/dt) \times (M/V_0) \times (P/P_0) \times (273 + T)/273 \times H \quad (1)$$

where F represents the gaseous PH_3 emission flux (ng m^{-2}·h^{-1}); dC/dt is the slope of the linear regression for the PH_3 concentration gradient over time (nmol·mol^{-1}·min^{-1}); M is the relative molecular mass of PH_3 (g·mol^{-1}); V_0 is the standard molar volume of gas (mL·mol^{-1}); P and P_0 are the atmospheric pressure in the chamber and standard atmospheric pressure (Pa), respectively; T is the atmospheric temperature during sampling (K); H is the effective height of chamber (m).

An acidic digestion method was applied to analyze the MBP (Han et al., 2000). Briefly, the fresh substrate samples (1 g) were digested in a self-made glass reactor with 5 mL 0.5 mol·L^{-1} sulfuric acid under an N_2 atmosphere (5 min, 55 °C). The liberated gaseous PH_3 was collected into a syringe and analyzed by GC as described above.

The multiple phase equilibration technique was applied to analyze dissolved PH_3 (Niu et al., 2004). Briefly, a 30-mL water sample and 20-mL N_2 were extracted into a syringe and then shaken for 2 min to reach equilibration for PH_3 extraction. Finally, the extracted $PH_3$was detected by GC as described above. The concentration of dissolved PH_3 was calculated according to Henry's law.

2.4. Physicochemical analysis

TP, NH_4^+-N, nitrate-nitrogen (NO_3^--N), nitrite-nitrogen (NO_2^--N) and COD, were analyzed every four days according to standard methods (APHA, 2012). The dissolved oxygen (DO) and redox potential (Eh) were measured *in situ* with multiparameter electrochemical analyzer (Hach, HQ40d, Colorado, USA).

Substrates samples from different layers in the CWs were collected at the end of the experiment (Li et al., 2021). The P fractions were analyzed using a modified Hedley sequential extraction method (Huett et al., 2005). The sequential extractions were performed with a solid-to-liquid ratio of 0.5 g: 30 mL. Resin-P was obtained by extracting the substrates with H_2O and anion exchange membranes saturated with a $NaHCO_3$ solution, $NaHCO_3$-P was obtained by extracting the substrates with 0.5 mol·L^{-1} $NaHCO_3$, NaOH-P was obtained by extracting the substrates with 0.1 mol·L^{-1} NaOH, HCl-P was obtained by extracting the substrates with 1.0 mol·L^{-1} HCl. Each extraction was performed under continuous shaking for 16 h. Following extraction, each suspension was centrifuged, and then the supernatants were taken for analysis. The residues were digested with hydrogen peroxide and sulfuric acid for residual-P analysis.

The P mass balance in CWs was calculated by the following equations (Nguyen et al., 2020):

$$L_{in} = C_{in} \times HLR = C_{in} \times Q/A = (C_{in} \times V_{in})/(A \times HRT) \tag{2}$$

$$L_{out} = C_{out} \times HLR = C_{out} \times Q/A = (C_{out} \times V_{out})/(A \times HRT) \tag{3}$$

$$\Delta m = L_{in} - L_{out} = (C_{in} \times V_{in} - C_{out} \times V_{out})/(A \times HRT) \tag{4}$$

where Δm is the TP removal rate (gP·m^{-2}·d^{-1}); $L_{in/out}$ is the P loading rates of the inflow and outflow (gP·m^{-2}·d^{-1}), respectively; $C_{in/out}$ is the P concentration of inflow and outflow (gP·m^{-2}·d^{-1}), respectively; $V_{in/out}$ is the wastewater volume of inflow and outflow (m^3), respectively; Q is the inlet flow (m^3·d^{-1}); A is the CW area (m^2); HRT is the hydraulic retention time (d).

If the different pathway of P is considered, the Δm can be calculated by the following equations:

$$\Delta m = R_{matrix\ sorption} + R_{plant\ uptake} + R_{phosphine\ emission} + R_{others} \tag{5}$$

$$R_{matrix\ sorption} = (C_{matrix} \times M_{matrix})/(A \times T) \tag{6}$$

$$R_{Plant\ uptake} = (C_{plant} \times M_{plant})/(A \times T) \tag{7}$$

$$R_{phosphine\ emission} = N_{phosphine}/(A \times T) \tag{8}$$

$$R_{others} = \Delta m - R_{matrix\ sorption} - R_{plant\ uptake} - R_{phosphine\ emission} \tag{9}$$

where C_{matrix} and C_{plant} are the P contents in the matrix after use and in the plant after harvest from CWs (g·kg^{-1}), respectively; M_{matrix} and M_{plant} are the mass of the matrix and plant (kg), respectively; $N_{phosphine}$ is the PH_3 released during the whole operation time of CWs (g); T is the whole operation time of CWs (d).

2.5. Microbial analysis

Samples from different depths of the CWs were taken at the end of the experiment and subjected to Illumina HiSeq sequencing of 16S rRNA. Genomic DNA was extracted using a DNA isolation kit (MoBio Laboratories, Inc., Carlsbad, CA, USA) according to the manufacturer's instructions. The V4 hypervariable region of the 16S rRNA gene was amplified with the primers 515F and 806R (Caporaso et al., 2011). The amplicons were purified, followed by sequencing on an Illumina Hiseq2500 platform at Novogene Bioinformatics Technology Co., Ltd. (Tianjin, China).

The nicotinamide adenine dinucleotide (NADH) content was quantified using assay kits obtained from Shanghai Enzyme-linked Biotechnology Co., Ltd. The specific test steps were performed according to the kit instructions.

2.6. Statistical analysis

All mathematical calculations of the raw data were performed in Excel 2019 (Microsoft office 2019, Microsoft, USA). Statistical analyses were performed using SPSS 22 (SPSS Inc., USA). All assays were performed in triplicate and were evaluated as significant based on a P value less than 0.05. The figures were generated with Origin 2018 (OriginLab, USA).

3. Results and discussion

3.1. Pollutants removal performance of constructed wetlands

Fig. 1 shows the pollutants removal efficiencies of different CWs. The COD removal efficiencies of CW-C and CW-P were 91.88% and 91.41%, respectively. The COD concentration of CW-P (17. 46 ± 1.26 mg·L^{-1}) was slightly higher than that of CW-C (16. 51 ± 3.33 mg·L^{-1}), mainly due to the degradation of PLA, as concave cavities induced by microbial corrosion could be observed on the surface of PLA granules at the end of the experiment (Fig. S1). The NH_4^+-N removal

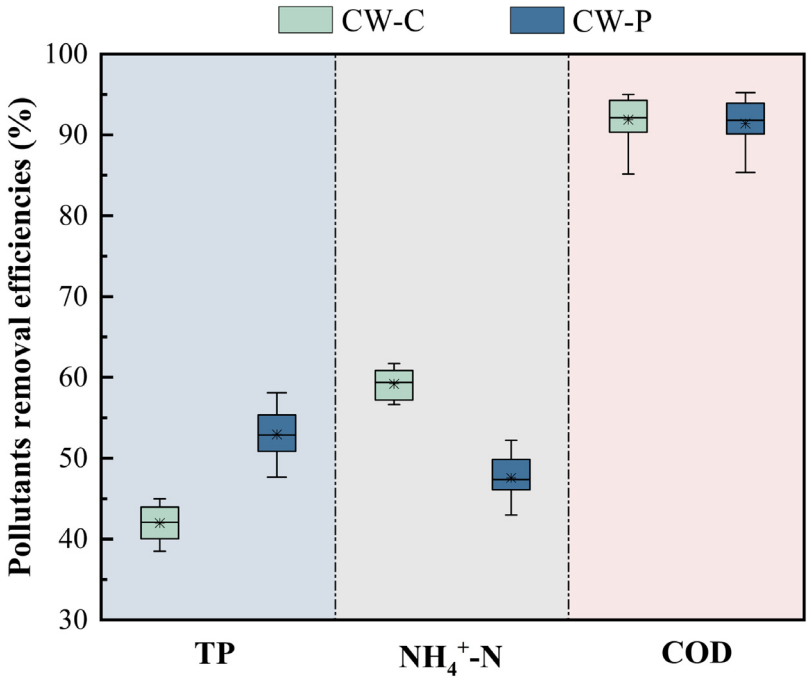

Fig. 1. Average removal efficiencies of total phosphorus (TP), ammonia-nitrogen (NH_4^+-N) and chemical oxygen demand (COD) in different constructed wetlands. The values of median, upper quartile, and the lower quartile are presented as the box.

efficiencies of CW-C and CW-P were 59.21% and 47.58%, respectively. Nitrification is the primary process to remove NH_4^+-N from CWs, but nitrification could be restrained by DO (Ding et al., 2016). CWs with high DO (6 mg·L^{-1}) by nozzle spray aeration could achieve an NH_4^+-N removal efficiency of 99.52% (Al-Wahaibi et al., 2021). The addition of PLA promoted competition among heterotrophic bacteria for DO and affected nitrification, so the NH_4^+-N removal efficiency in CW-P was lower than that in CW-C. The TP removal efficiency of CW-P was 52.96% higher than that of CW-C (41.99%). This result occurred because the addition of PLA optimized the migration and transformation of P in CW-P, thereby improving its P removal efficiency. For a detailed analysis, please refer to Section 3.3.

3.2. Characteristic presence of phosphine in constructed wetlands

Generally, the PH_3 in CWs exists in three forms, i.e., dissolved PH_3, gaseous PH_3, and matrix-bound PH_3. The average concentrations of dissolved PH_3 in CW-P and CW-C were 4.08 $\pm$0.96 μg·L^{-1} and 2.73 $\pm$0.62 μg·L^{-1}, respectively. Phosphine from different sources is shown in Table 1. Niu et al. (2004) found that the dissolved PH_3 in Taihu Lake ranged from 1.92 to 3.01 pg·L^{-1}, which is much lower than that in CW-P and CW-C. CWs are often in an anaerobic or anoxic state, and the phosphate concentration in the interstitial water of the CW is much higher than that in the lake (0.09–0.26 mg·L^{-1}), which is conducive to the reduction of phosphate to PH_3. PH_3 released into water bodies can stimulate the growth of *Thalassiosira pseudonana* by promoting the expression and activity of phosphate transporter genes (Fu et al., 2013). Given the relatively low critical concentration of P that produced eutrophication (i.e., 10–20 μg·L^{-1}), the dissolved PH_3 and its oxides in the effluent could promote cyanobacterial bloom outbreaks (Sheng et al., 2019), and the role of dissolved PH_3 in the effluent of the CW may have been underestimated.

Fig. 2a shows the gaseous PH_3 release flux during a typical cycle. The PH_3 release fluxes of CW-P and CW-C were 220.50 $\pm$ 25.40 pg·m^{-2}·h^{-1} and 139.99 $\pm$ 13.91 pg·m^{-2}·h^{-1}, respectively (Eq. (1)). At the beginning of the flooding phase, phosphate was mainly adsorbed and precipitated on the substrates, and the redox potential of the CW was greater than 150 mV (Fig. 2b). PH_3 is a potent reducing agent, and a higher redox potential is disadvantageous for the production and preservation of PH_3 (Chen et al., 2017). With the increase in submersion, the redox potential decreased, and the reducing environment gradually emerged in the CWs. Thus, the production and preservation of PH_3 were guaranteed, and the release of gaseous PH_3 was detected at the later stage of the flooding period. Moreover, the flux of PH_3 in CWs was higher than that at the lake sediment-water interface, but lower than that in the paddy fields (Table 1). Diffusion resistance in different environments impedes the emission of PH_3 (Niu et al., 2013).

MBP is the main form of PH_3 in CWs. The average concentrations of MBP in CW-C and CW-P were 6.15 ng·kg^{-1} and 13.06 ng·kg^{-1}, respectively. As a high-energy electron donor, PLA might strengthen the phosphate reduction to PH_3. The vertical distribution characteristics of MBP in CWs are shown in Fig. 3. The MBP concentration increased with increasing

Table 1
Phosphine from different sources.

Form	Source	Concentration	Reference
Free gaseous phosphine	Louisiana brackish marsh	0.42–6.52 $ng{\cdot}m^{-2}{\cdot}h^{-1}$	Devai and Delaune (1995)
	Sediment-water Interface	13.8 ± 5 $pg{\cdot}m^{-2}{\cdot}h^{-1}$	Geng et al. (2005)
	Coastal Antarctica	30–407.8 $ng{\cdot}m^{-3}$	Zhu et al. (2006)
	Yancheng marsh	(−227 ± 57)–(276 ± 100) $ng{\cdot}m^{-2}{\cdot}h^{-1}$	Han et al. (2011c)
	Lake Taihu	37.0 ± 22.7 $ng{\cdot}m^{-3}$	Han et al. (2011c)
	Coastal zone of yellow sea	1.71 ± 0.73 $ng{\cdot}m^{-3}$	Han et al. (2011c)
	Paddy fields	(−4.92 ± 2.26)–(14.40 ± 0.97) $ng{\cdot}m^{-2}{\cdot}h^{-1}$	Chen et al. (2017)
Dissolved phosphine	Hamburg Harbour	(0.2 ± 0.03)–(12.5 ± 1.9) $nM{\cdot}dm^{-3}$	Gassmann (1994)
	Taihu Lake water	1.92–3.01 $pg{\cdot}L^{-1}$	Niu et al. (2004)
Matrix bound phosphine	Taihu Lake sediment	5–919 $ng{\cdot}kg^{-1}$	Niu et al. (2004)
	Sediment of coastal Antarctica	1.57–3.04 $ng{\cdot}kg^{-1}$	Zhu et al. (2006)
	Sediment of coastal China	0.89–25.86 $ng{\cdot}kg^{-1}$	Feng et al. (2008)
	Paddy soils	0–7 $ng{\cdot}kg^{-1}$	Han et al. (2000)
	Paddy soils	(18.28 ± 3.74)–(211.73 ± 42.01) $ng{\cdot}kg^{-1}$	Chen et al. (2017)

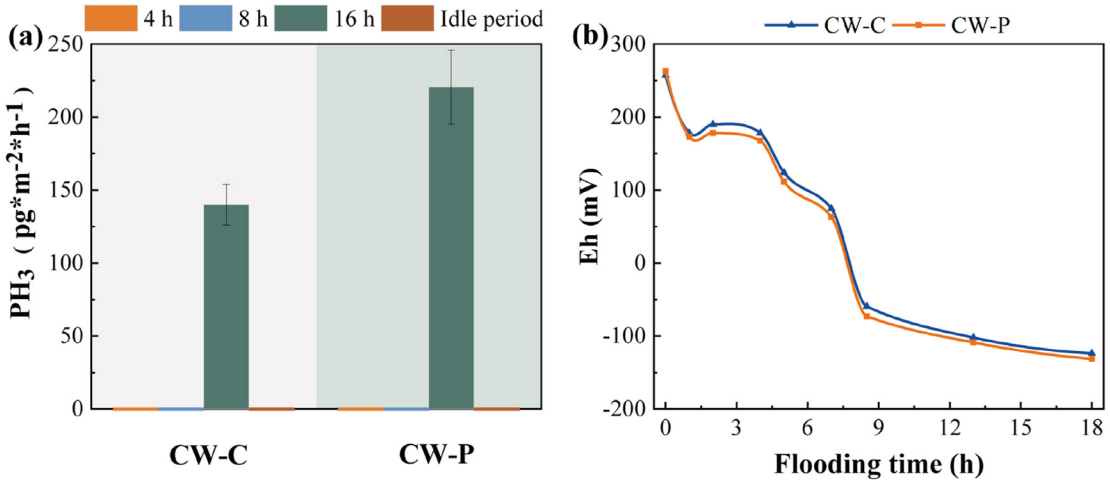

Fig. 2. Variation of phosphine (PH_3) release flux (a) and redox potential (Eh) (b) in a typical period.

matrix depth, and the maximum MBP concentration was observed at the bottom layer (60–75 cm) of the matrix in both CWs (13.70 ± 2.31 $ng{\cdot}kg^{-1}$ and 16.39 ± 2.64 $ng{\cdot}kg^{-1}$, respectively). PH_3 in the surface layer can be easily oxidized to phosphates or released into the atmosphere, which explains the its low concentration of MBP. However, the reduction condition at the bottom layer of the CWs is superior to that at the surface layer, and is conducive to the production and preservation of PH_3. Moreover, MBP is similar to a repository of PH_3, which can be converted to gaseous PH_3 and dissolved PH_3. Gaseous PH_3 and dissolved PH_3 undergo multiple sorption, desorption, and even oxidation processes when they migrate inside CWs. The migration and transformation of gaseous PH_3 play an important role in the P cycle and stimulate P removal in CWs.

3.3. Effect of phosphine on phosphorus transformation in constructed wetlands

The phosphorus flow rates ($gP{\cdot}m^{-2}{\cdot}d^{-1}$) of different routes in CWs are shown in Table 2. The plant uptake rates of P in CW-C and CW-P were 0.016 $gP{\cdot}m^{-2}{\cdot}d^{-1}$ and 0.020 $gP{\cdot}m^{-2}{\cdot}d^{-1}$, respectively (Eq. (7)). Similar results have also been reported: *Cyperus papyrus* (0.014 $gP{\cdot}m^{-2}{\cdot}d^{-1}$), *Phragmites australis* (0.032 $gP{\cdot}m^{-2}{\cdot}d^{-1}$), and *Potamogeton pectinatus* (0.011 $gP{\cdot}m^{-2}{\cdot}d^{-1}$) (Luo et al., 2017). However, compared with CW-C, the plant uptake rate of P in CW-P was higher. Wang et al. (2016) found that the plant P uptake capacity of rice seedlings could be increased under PH_3 treatment. Oxygen transport from plants to the rhizosphere could cause PH_3 to transform back to phosphate, which can be easily utilized by plants and microorganisms.

The matrix had a significant effect on P removal in CWs. P sorption of the matrix in CWs accounted for 30.20–58.86% of its P removal, much higher than those of plant uptake and PH_3 emissions, indicating that matrix sorption dominated the P removal pathway of CWs. The P sorption of the matrix was 0.342 $gP{\cdot}m^{-2}{\cdot}d^{-1}$ in CW-P, which was much higher than that in CW-C (0.168 $gP{\cdot}m^{-2}{\cdot}d^{-1}$) (Eq. (6)). This result can be explained by the difference in P fractions between CW-P and CW-C (Fig. 4). In CW-C, the percentages of P fractions declined in the following order: HCl-P (41.07–50.97%) > NaOH-P

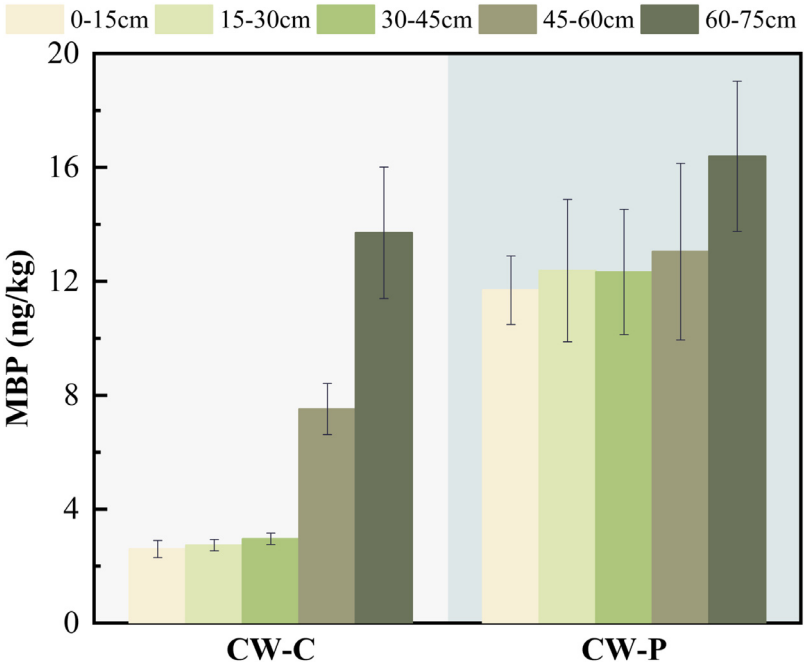

Fig. 3. The concentrations of matrix-bound phosphine (MBP) in different depths of constructed wetlands.

Table 2
Phosphorus flow rates ($gP{\cdot}m^{-2}{\cdot}d^{-1}$) of different routes in constructed wetlands.

CW	Influent	Effluent	Plant uptake	Matrix sorption	Gaseous PH_3	Dissolved PH_3	Others
CW-C	1.582 ± 0.013	1.125 ± 0.024	0.016 ± 0.001	0.168 ± 0.006	$(3.07 \pm 0.86) \times 10^{-9}$	$(6.63 \pm 1.02) \times 10^{-4}$	0.276 ± 0.037
CW-P	1.582 ± 0.013	1.001 ± 0.019	0.020 ± 0.001	0.342 ± 0.014	$(4.82 \pm 0.99) \times 10^{-9}$	$(1.10 \pm 0.53) \times 10^{-3}$	0.225 ± 0.029

(32.20–38.39%) > $NaHCO_3$-P (8.65–13.30%) > Resin-P (3.86–9.29%). The same order observed in CW-P: HCl-P (29.56–44.00%) > NaOH-P (25.06–34.41%) > $NaHCO_3$-P (21.91–24.23%) > Resin-P (8.54–13.65%), which is consistent with the results reported by Si et al. (2021). The availability of P fractions for organisms is as follows: Resin-P and $NaHCO_3$(readily organism-available P) > NaOH-P (moderately available, Al-Fe-associated P) > HCl-P (slowly available, Ca-Mg-associated P) (Ashjaei et al., 2010). Moreover, compared with CW-C, the proportion of readily organism-available P in CW-P was increased, and the proportions of Al-Fe-associated P and Ca-Mg-associated P were decreased. Han et al. (2011b) suggested that Ca-associated P mainly affects MBP production in paddy soils. The generation of a high concentration of MBP in CW-P was accompanied by Ca-P consumption. In other words, microorganisms could use Ca-P to produce PH_3. As PH_3 migrated in CWs, it would be adsorbed by the matrix or oxidized to phosphate and transformed into loosely bound P: Resin-P, $NaHCO_3$, and MBP. Therefore, after the conversion of PH_3, the proportion of available P increased, and the ion-bound phosphates decreased. Except for the change in phosphorus fractions, the matrix P adsorption capacity of CW-P was twice that of CW-C. The adsorption of P by the matrix is mainly through physical and chemical effects, in which the binding between ions (i.e., Ca^{2+}, Mg^{2+}, Al^{3+}, and Fe^{2+}) and P is the most stable combination. Nevertheless, these chemical binding sites tend to become saturated over time, and the adsorption capacity for P by the matrix declines. Even phosphorus desorption occurs. However, the production process of PH_3 can utilize the ion bound P, causing the chemical binding sites to be released; therefore, the phosphate in sewage can be adsorbed efficiently and sharply during the initial flooding period (Fig. S2). CW-P had a higher phosphate adsorption capacity than CW-C due to having more chemical binding sites. It was found that the TP concentration increased slightly with the increase in flooding time, which could represent the release of endogenous phosphorus from microorganisms, or the desorption of loosely bound phosphates by microorganisms. The transformation of phosphate at the matrix interface requires more detailed research.

In addition to matrix sorption and plant uptake, the PH_3 emission from the CWs could not be ignored. PH_3 emission includes the gaseous PH_3 release and dissolved PH_3 discharge from the CWs. The dissolved PH_3 discharged from CW-C and CW-P was 6.63×10^{-4} $gP{\cdot}m^{-2}{\cdot}d^{-1}$ and 1.10×10^{-3} $gP{\cdot}m^{-2}{\cdot}d^{-1}$, respectively, which accounted for 0.14–0.20% of the P removed in CWs (Eq. (8)). Although the release of gaseous PH_3 in CWs was minor, its migration and transformation in CWs are irreplaceable for the P cycle and removal. Moreover, the PH_3 released into the environment will also have a certain impact. For example, the migration of PH_3 to phosphorus-limited areas could promote the growth of biomass (positive aspect: promoting crop growth; negative aspect: causing algal blooms or eutrophication.). In addition, PH_3 in the atmosphere could react with ozone and indirectly enhance the greenhouse effect (Fu and Zhang, 2020).

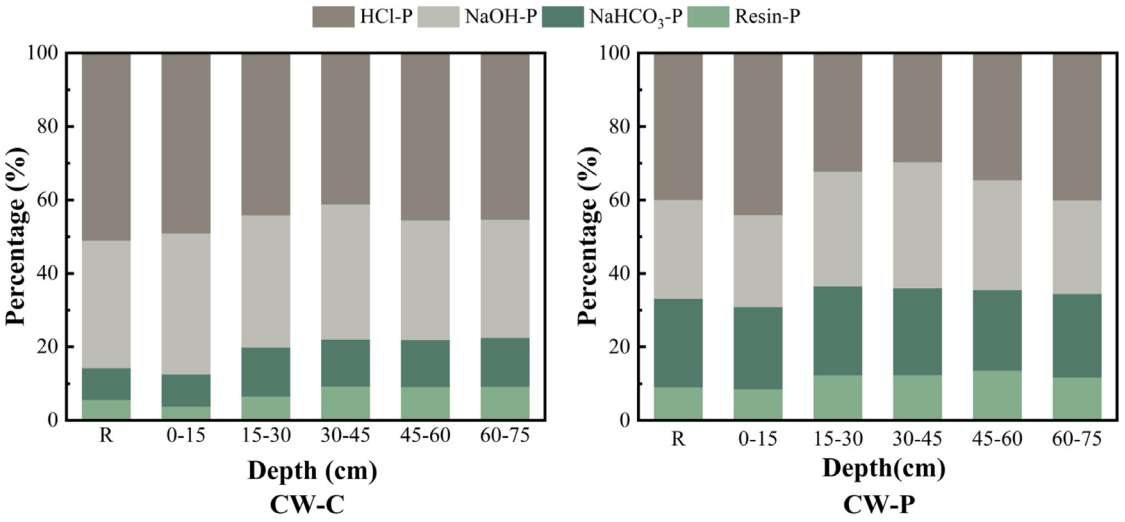

Fig. 4. The percentages of phosphorus binding forms in different layers of constructed wetlands.

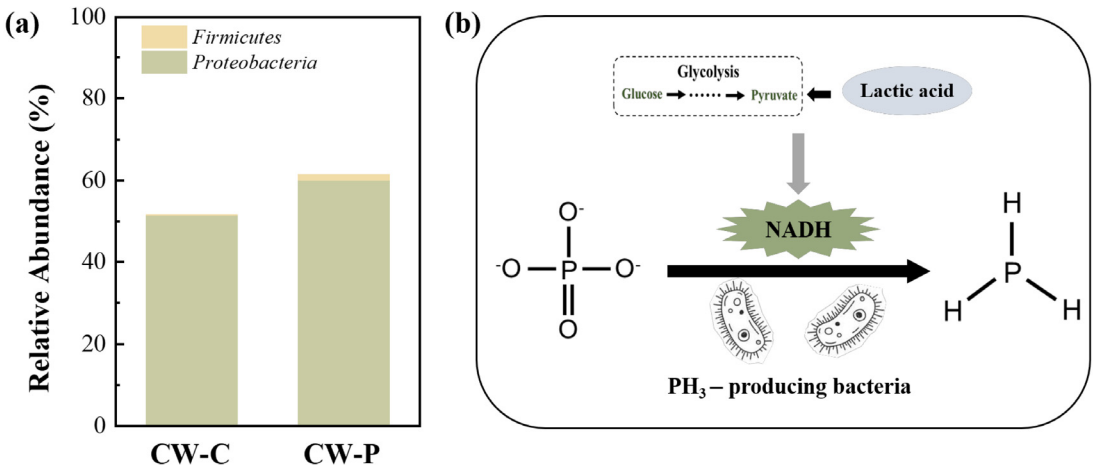

Fig. 5. The relative abundance of phosphine-producing bacteria (a) and the illustration of phosphate reduction process (b) in constructed wetlands.

In summary, plant uptake, matrix adsorption and PH_3 transformation all contributed to phosphorus removal in CWs. Matrix adsorption had a significant effect on P removal in CWs, and PH_3 formation and transformation in CWs released chemical binding sites of the matrix; thus, the phosphate adsorption capacity was enhanced. However, a more comprehensive understanding and evaluation of PH_3 is needed.

3.4. Mechanism of phosphine production in wetlands

Some studies have identified microorganisms that could produce PH_3. Jenkins et al. (2000) found that some mixed-culture anaerobic microorganisms (butyric acid fermentation bacteria) and purebred microorganisms (*Escherichia coli*, *Salmonella gallinarum*, *Clostridium sporogenes*, etc.) were able to generate PH_3. Fan et al. (2020a, 2021) found that *Ruminococcaceae* which can degrade organic matter into small organic acids, contributed to the production of PH_3. *Azotobacter*, with its hydrogen-producing functions, could provide an electron donor for the production of PH_3. The PH_3-producing bacteria mentioned above were mainly concentrated in *Firmicutes* and *Proteobacteria*, which were also observed in both CWs (Fig. 5a). The relative abundance of PH_3-producing bacteria in CW-P was 9.8% higher than that in CW-C, which benefits PH_3 production.

Thermodynamic analysis showed that phosphate reduction is a nonspontaneous reaction, indicating that polylactic acid added to CW-P did not directly participate in phosphate reduction as an electron donor (Table S2). Regardless, it is well known that some thermodynamically nonspontaneous reactions such as nitrogen fixation can occur in nature under

the effects of microorganisms and enzymes. Therefore, it is speculated that some specific bacteria and enzymes might be involved in the reduction of phosphate in CWs.

However, *Enterobacter* can produce more PH_3 under the influence of NADH (Fan et al., 2020b). It is well known that, the degradation and hydrolysis of PLA granules can drive the reversible reaction ($pyruvate + NADH + H^+ \leftrightarrow NAD^+ + lactate$) towards the formation of pyruvate accompanied by NADH generation (Jia et al., 2018). The results also showed that the NADH concentration of CW-P was 44.03 $ng \cdot kg^{-1}$, which is 13.77% higher than that of CW-C (Table S3). Thus, it is suggested that PH_3-producing bacteria such as *Proteobacteria* and *Firmicutes* could reduce phosphates to PH_3, and that NADH (generated from glycolysis, the reversible reaction between lactic acid and pyruvate) catalyzes this reduction process (Fig. 5b). This explains why more PH_3 was produced in CW-P under the effect of PH_3-producing bacteria and NADH.

4. Conclusions and future directions

This study suggests that MBP was the dominant form of PH_3 in CWs, and the formation and migration of PH_3 in CWs had a significant effect on P removal. PH_3 increased the proportion of available P and subsequently improved the P adsorption capacity of the matrix by 103.6%. Thus, the TP removal efficiency of CW-P was increased by 10.97%. Microbial analysis revealed that PH_3-producing bacteria, including *Proteobacteria* and *Firmicutes*, could reduce phosphates to PH_3 under the catalysis of NADH. These results are of considerable significance for the long-term and stable operation of CWs, as they provided a new pathway to realize phosphorus removal and overcome the limitation of the matrix absorption capacity. However, further study is needed to reveal the transformation of phosphate at the matrix interface. Optimization of the structure and operation mode of CWs needs to be conducted to improve gaseous PH_3 release from CWs to realize high efficiency "dephosphorization by gasification".

CRediT authorship contribution statement

Shuo Wang: Conceptualization, Writing – reviewing and editing. **Zhen Hu:** Supervision. **Jian Zhang:** Investigation. **Haiming Wu:** Writing – reviewing and editing. **Huijun Xie:** Data curation, Visualization. **Shuang Liang:** Data curation, Visualization. **Haodong Hu:** Writing – original draft. **Fenglin Jin:** Methodology, Software.

Declaration of competing interest

The authors declare that they have no known competing financial interests or personal relationships that could have appeared to influence the work reported in this paper.

Acknowledgments

This work was supported by the National Natural Science Foundation of China (No. 51878388 & No. 52170043); the Natural Science Foundation of Shandong Province, PR China (No. ZR2020YQ42); the Shandong Provincial Key Research and Development Program (Major Scientific and Technological Innovation Project), PR China (No. 2020CXGC011406 & No. 2019JZZY010411); and the Future Plan for Young Scholar of Shandong University, PR China.

Appendix A. Supplementary data

Supplementary material related to this article can be found online at https://doi.org/10.1016/j.eti.2022.102653.

References

Al-Wahaibi, B.M., Jafary, T., Al-Mamun, A., Baawain, M.S., Aghbashlo, M., Tabatabaei, M., Stefanakis, A.I., 2021. Operational modifications of a full-scale experimental vertical flow constructed wetland with effluent recirculation to optimize total nitrogen removal. J. Clean. Prod. 296, 126558.

APHA, 2012. Standard Methods for the Examination of Water and Wastewater, twenty-first ed. American Public Health Association, American Water Works Association & Water Environment Federation, New York.

Arias, C.A., Del Bubba, M., Brix, H., 2001. Phosphorus removal by sands for use as media in subsurface flow constructed reed beds. Water Res. 35 (5), 1159–1168.

Ashjaei, S., Tiessen, H., Schoenau, J.J., 2010. Correlations between phosphorus fractions and total leachate phosphorus from cattle manure- and swine manure-amended soil. Commun. Soil Sci. Plan. 41 (11), 1338–1349.

Blanco, I., Molle, P., de Miera, L.E.S., Ansola, G., 2016. Basic oxygen furnace steel slag aggregates for phosphorus treatment, evaluation of its potential use as a substrate in constructed wetlands. Water Res. 89, 355–365.

Caporaso, J.G., Lauber, C.L., Walters, W.A., Berg-Lyons, D., Lozupone, C.A., Turnbaugh, P.J., Fierer, N., Knight, R., 2011. Global patterns of 16s rRNA diversity at a depth of millions of sequences per sample. Proc. Natl. Acad. Sci. U.S.A. 108, 4516–4522.

Chen, W., Niu, X., An, S., Sheng, H., Tang, Z., Yang, Z., Gu, X., 2017. Emission and distribution of phosphine in paddy fields and its relationship with greenhouse gases. Sci. Total Environ. 599–600, 952–959.

Devai, I., Delaune, R.D., 1995. Evidence for phosphine production and emission from louisiana and florida marsh soils. Org. Geochem. 23 (3), 277–279.

Devai, I., Felfoldy, L., Wittner, I., Plosz, S., 1988. Detection of phosphine - new aspects of the phosphorus cycle in the hydrosphere. Nature 333 (6171), 343–345.

Ding, Y., Wang, W., Liu, X.P., Song, X.S., Wang, Y.H., Ullman, J.L., 2016. Intensified nitrogen removal of constructed wetland by novel integration of high rate algal pond biotechnology. Bioresour. Technol. 219, 757–761.
Ding, L., Wang, X., Zhu, Y., Edwards, M., Glindemann, D., Ren, H., 2005. Effect of pH on phosphine production and the fate of phosphorus during anaerobic process with granular sludge. Chemosphere 59 (1), 49–54.
Drizo, A., Comeau, Y., Forget, C., Chapuis, R.P., 2002. Phosphorus saturation potential: A parameter for estimating the longevity of constructed wetland systems. Environ. Sci. Technol. 36 (21), 4642–4648.
Eismann, F., Glindemann, D., Bergmann, A., Kuschk, P., 1997. Soils as source and sink of phosphine. Chemosphere 35 (3), 523–533.
Fan, Y.M., Lv, M.Y., Niu, X.J., Ma, J.L., Song, Q., 2020b. Evidence and mechanism of biological formation of phosphine from the perspective of the tricarboxylic acid cycle. Int. Biodeterior. Biodegrad 146, 104791.
Fan, Y., Lv, M., Niu, X., Ma, J., Zhang, D., 2020a. The key step of gaseous phosphorus release in anaerobic digestion. Process. Saf. Environ. 137, 238–245.
Fan, Y.M., Niu, X.J., Zhang, D.Q., Lin, Z., Fu, M.L., Zhou, S.Q., 2021. Analysis of the characteristics of phosphine production by anaerobic digestion based on microbial community dynamics, metabolic pathways, and isolation of the phosphate-reducing strain. Chemosphere 262, 128213.
Feng, Z.H., Song, X.X., Yu, Z.M., 2008. Distribution characteristics of matrix-bound phosphine along the coast of China and possible environmental controls. Chemosphere 73 (4), 519–525.
Fu, M., Song, X., Yu, Z., Liu, Y., 2013. Responses of phosphate transporter gene and alkaline phosphatase in thalassiosira pseudonana to phosphine. PLoS One 8 (3), e59770.
Fu, W.Y., Zhang, X.H., 2020. Global phosphorus dynamics in terms of phosphine. NPJ Clim. Atmos. Sci. 3 (1), 51.
Gassmann, G., 1994. Phosphine in the fluvial and marine hydrosphere. Mar. Chem. 45 (3), 197–205.
Geng, J.J., Niu, X.J., Jin, X.C., Wang, X.R., Gu, X.H., Edwards, M., Glindemann, D., 2005. Simultaneous monitoring of phosphine and of phosphorus species in Taihu lake sediments and phosphine emission from lake sediments. Biogeochemistry 76 (2), 283–298.
Glindemann, D., Edwards, M., Kuschk, P., 2003. Phosphine gas in the upper troposphere. Atmos. Environ. 37 (18), 2429–2433.
Glindemann, D., Edwards, M., Morgenstern, P., 2005. Phosphine from rocks: mechanically driven phosphate reduction? Environ. Sci. Technol. 39 (21), 8295–8299.
Han, C., Geng, J.J., Hong, Y.N., Zhang, R., Gu, X.Y., Wang, X.R., Gao, S.X., Glindemann, D., 2011c. Free atmospheric phosphine concentrations and fluxes in different wetland ecosystems, China. Environ. Pollut. 159 (2), 630–635.
Han, C., Geng, J.J., Zhang, J., Wang, R., Gao, S.X., 2011a. Phosphine migration at the water-air interface in Lake Taihu, China. Chemosphere 82 (6), 935–939.
Han, C., Geng, J.J., Zhang, R., Wang, X.R., Gao, S.X., 2011b. Matrix-bound phosphine and phosphorus fractions in paddy soils. J. Environ. Monit. 13 (4), 844–849.
Han, S.H., Zhuang, Y.H., Liu, J.A., Glindemann, D., 2000. Phosphorus cycling through phosphine in paddy fields. Sci. Total Environ. 258 (3), 195–203.
Han, S.H., Zhuang, Y.H., Zhang, H.X., Wang, Z.J., Yang, J.Z., 2002. Phosphine and methane generation by the addition of organic compounds containing carbon-phosphorus bonds into incubated soil. Chemosphere 49 (6), 651–657.
Huett, D.O., Morris, S.G., Smith, G., Hunt, N., 2005. Nitrogen and phosphorus removal from plant nursery runoff in vegetated and unvegetated subsurface flow wetlands. Water Res. 39 (14), 3259–3272.
Jenkins, R.O., Morris, T.A., Craig, P.J., Ritchie, A.W., Ostah, N., 2000. Phosphine generation by mixed- and monoseptic-cultures of anaerobic bacteria. Sci. Total Environ. 250 (1–3), 73–81.
Jia, B.L., Pu, Z.J., Tang, K., Jia, X.M., Kim, K.H., Liu, X.L., Jeon, C.O., 2018. Catalytic, computational, and evolutionary analysis of the D-lactate dehydrogenases responsible for D-lactic acid production in lactic acid bacteria. J. Agric. Food Chem. 66 (31), 8371–8381.
Li, M., Duan, R., Hao, W., Li, Q.C., Liu, P.P., Qi, X., Huang, X., Shen, X.Q., Lin, R.F., Liang, P., 2021. Utilization of elemental sulfur in constructed wetlands amended with granular activated carbon for high-rate nitrogen removal. Water Res. 195, 116996.
Luo, P., Liu, F., Liu, X.L., Wu, X., Yao, R., Chen, L., Li, X., Xiao, R.L., Wu, J.S., 2017. Phosphorus removal from lagoon-pretreated swine wastewater by pilot-scale surface flow constructed wetlands planted with *Myriophyllum aquaticum*. Sci. Total Environ. 576, 490–497.
Nguyen, T.A.H., Ngo, H.H., Guo, W.S., Nguyen, T.H.H., Soda, S., Vu, N.D., Bui, T.K.A., Vo, T.D.H., Bui, X.T., Nguyen, T.T., Pham, T.T., 2020. White hard clam (*Meretrix lyrata*) shells media to improve phosphorus removal in lab-scale horizontal sub-surface flow constructed wetlands: Performance, removal pathways, and lifespan. Bioresour. Technol. 312, 123602.
Niu, X.J., Geng, J.J., Wang, X.R., Wang, C.H., Gu, X.H., Edwards, M., Glindemann, D., 2004. Temporal and spatial distributions of phosphine in Taihu Lake, China. Sci. Total Environ. 323 (1–3), 169–178.
Niu, X.J., Wei, A.S., Li, Y.D., Mi, L.N., Yang, Z.Q., Song, X.F., 2013. Phosphine in paddy fields and the effects of environmental factors. Chemosphere 93 (9), 1942–1947.
Pratt, C., Shilton, A., Haverkamp, R.G., Pratt, S., 2009. Assessment of physical techniques to regenerate active slag filters removing phosphorus from wastewater. Water Res. 43 (2), 277–282.
Roels, J., Huyghe, G., Verstraete, W., 2005. Microbially mediated phosphine emission. Sci. Total Environ. 338 (3), 253–265.
Shen, Z.Q., Zhou, Y.X., Liu, J., Xiao, Y., Cao, R., Wu, F.P., 2015. Enhanced removal of nitrate using starch/PCL blends as solid carbon source in a constructed wetland. Bioresour. Technol. 175, 239–244.
Sheng, H., Niu, X.J., Song, Q., Li, Y.K., Zhang, R.Y., Zou, D.H., Lai, S.C., Yang, Z.Q., Tang, Z.H., Zhou, S.Q., 2019. Physiological and biochemical responses of *Microcystis aeruginosa* to phosphine. Environ.l Pollut. 247, 165–171.
Si, Z.H., Song, X.S., Wang, Y.H., Cao, X., Wang, Y.F., Zhao, Y.F., Ge, X.Y., 2021. Natural pyrite improves nitrate removal in constructed wetlands and makes wetland a sink for phosphorus in cold climates. J. Clean. Prod. 280, 124304.
Vymazal, J., 2007. Removal of nutrients in various types of constructed wetlands. Sci. Total Environ. 380 (1–3), 48–65.
Wang, J.F., Li, L., Niu, X.J., Zou, D.H., 2016. Phosphine-induced phosphorus mobilization in the rhizosphere of rice seedlings. J. Soils Sediments 16 (6), 1735–1744.
Wang, R.G., Zhao, X., Wang, T.C., Guo, Z.Z., Hu, Z., Zhang, J., Wu, S.B., Wu, H.M., 2022. Can we use mine waste as substrate in constructed wetlands to intensify nutrient removal? A critical assessment of key removal mechanisms and long-term environmental risks. Water Res. 210, 118009.
Westholm, L.J., 2006. Substrates for phosphorus removal - potential benefits for on-site wastewater treatment? Water Res. 40 (1), 23–36.
Wu, H.M., Zhang, J., Ngo, H.H., Guo, W.S., Hu, Z., Liang, S., Fan, J.L., Liu, H., 2015. A review on the sustainability of constructed wetlands for wastewater treatment: Design and operation. Bioresour. Technol. 175, 594–601.
Xia, D., Yi, X.Y., Lu, Y., Huang, W.L., Xie, Y.Y., Ye, H., Dang, Z., Tao, X.Q., Li, L., Lu, G.N., 2019. Dissimilatory iron and sulfate reduction by native microbial communities using lactate and citrate as carbon sources and electron donors. Ecotox. Environ. Safe 174, 524–531.
Yang, Y., Zhao, Y.Q., Tang, C., Mao, Y., Chen, T.H., Hu, Y.S., 2021. Novel pyrrhotite and alum sludge as substrates in a two-tiered constructed wetland-microbial fuel cell. J. Clean. Prod. 293, 126087.
Yang, Z., Zhou, J., Li, J., Han, Y., He, Q., 2016. Pre-processing of raw wastewater in a septic tank leads to phosphorus removal by phosphine production in a sequencing batch biofilm reactor (SBBR). Desalin. Water Treat. 57 (2), 810–818.
Zhang, M., Chen, C., Zhou, S.Y., Yang, J.Q., Qiu, H., Zhao, D.H., An, S.Q., 2020. Operation strategy for constructed wetlands in dry seasons with insufficient influent wastewater. Bioresour. Technol. 317, 124049.

Zhang, X.W., Hu, Z., Ngo, H.H., Zhang, J., Guo, W.S., Liang, S., Xie, H.J., 2018. Simultaneous improvement of waste gas purification and nitrogen removal using a novel aerated vertical flow constructed wetland. Water Res. 130, 79–87.
Zhu, R.B., Kong, D.M., Sun, L.G., Geng, J.J., Wang, X.R., Glindemann, D., 2006. Tropospheric phosphine and its sources in coastal Antarctica. Environ. Sci. Technol. 40 (24), 7656–7661.
Zhu, R.B., Ma, D.W., Ding, W., Bai, B., Liu, Y.S., Sun, J.J., 2011. Occurrence of matrix-bound phosphine in polar ornithogenic tundra ecosystems: Effects of alkaline phosphatase activity and environmental variables. Sci. Total Environ. 409 (19), 3789–3800.